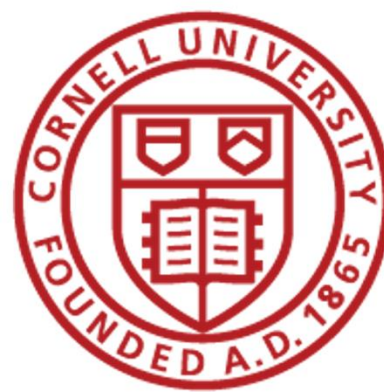


# Reduced Order Model of Neutral Particle Density In Electrospray Thruster Plumes

Maddox Nesterczuk

Advisor: Adler Smith



Neutral particles cause many problems for spacecraft:

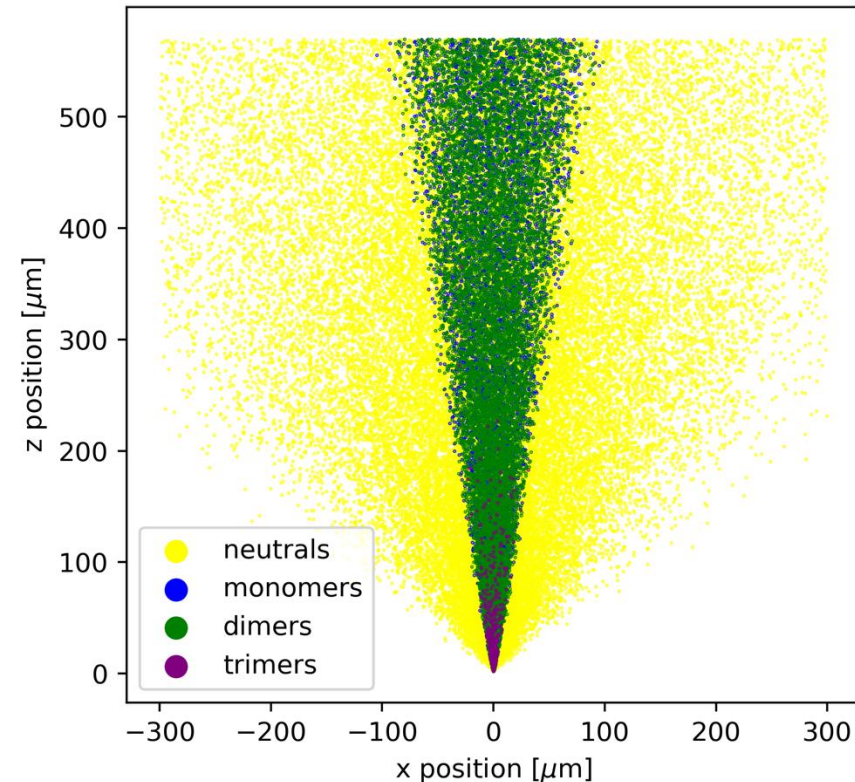


Figure 1. Simulation of plume behind a single emitter.

**Performance:** Neutrals are not accelerated by the electric field, so do not contribute to thrust

**Damage:** Neutral interactions with downstream surfaces from overspray leads to spacecraft damage

**Power:** Neutral accumulation on solar panels due to light scattering/absorption causes loss in power

No sufficiently researched model of spatial distribution of neutral particles behind single emitter/array.

# Research Questions

- How does the neutral density behind a single emitter/array vary with spatial location and operating conditions?
- How does voltage effect fragmentation behavior in the plume and thus the distribution of neutrals?
- What is the neutral density distribution behind an array of emitters?

# Mass Flux and Current Density Distributions of Electrospray Plumes

## Thuppul et al (2021)

Experimental data shows angular distribution of current density approximately supergaussian (Thuppul et al., 2021).

The Electrohydrodynamic (EHD) emission model suggests both On-axis and Off-axis emission sites.

Since neutrals are generated via fragmentation, the neutral distribution has two regions: Core and Wing

**Proposed Model:** Use a two-component gaussian model to describe the combined angular distribution of these two regions.

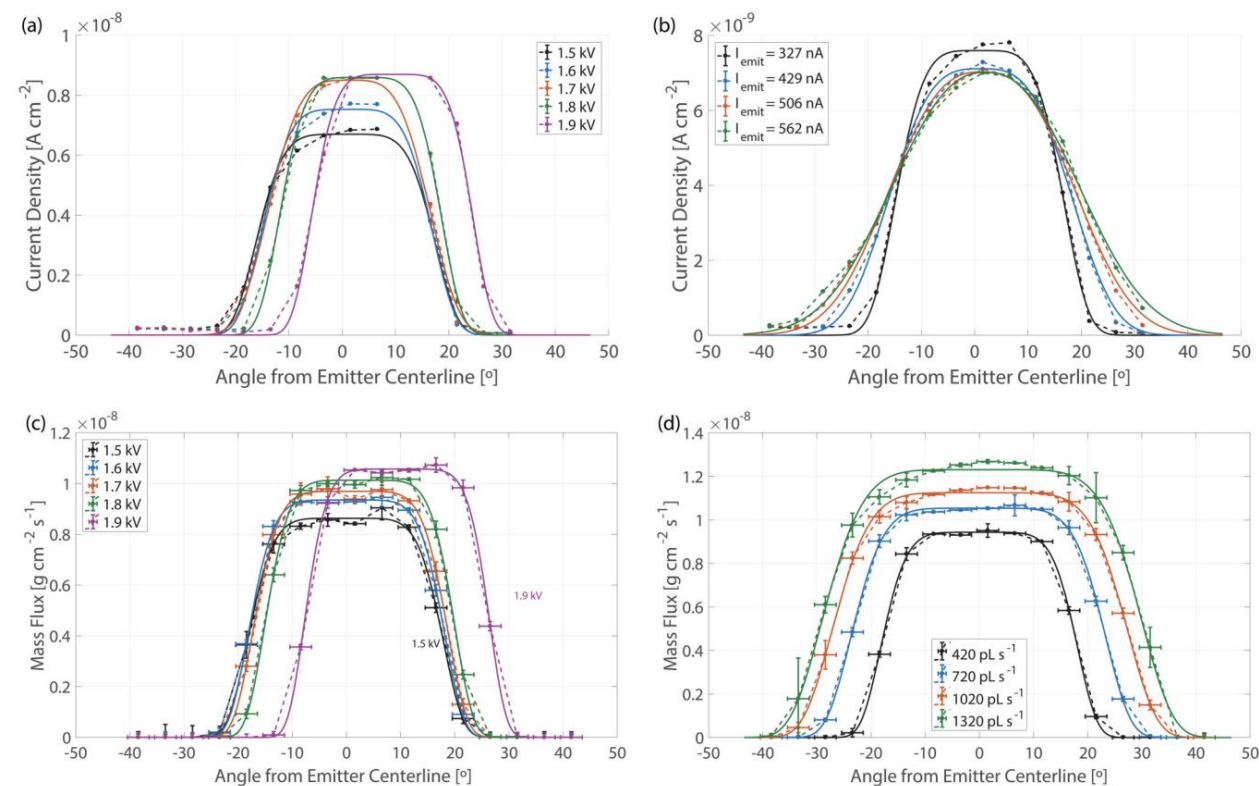


FIG. 3. Current density as a function of half angle for varying (a) extraction voltages (fixed flow rate of 420 pL s<sup>-1</sup>) and (b) flow rates (constant voltage of 1.6 kV). Mass flux as a function of half angle for varying (c) extraction voltages (fixed flow rate of 420 pL s<sup>-1</sup>) and (d) flow rates (constant voltage of 1.6 kV). All profiles shown with super-Gaussian fits. The trends of these fits with voltage and flow rates are shown in Fig. 5.

Figure 2. Experimental data of mass flux of ions approximately supergaussian. (Thuppul et al, 2021)

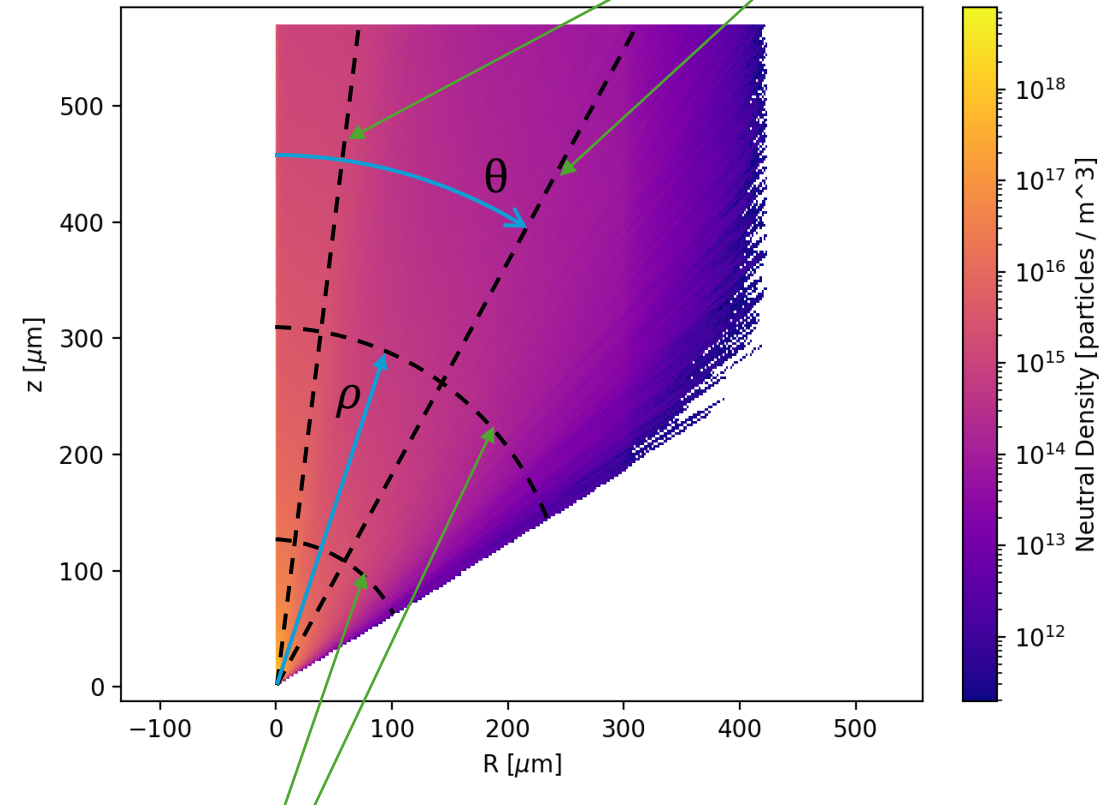
# Methodology: functional form for density profiles

$$D(\rho) = \frac{C}{\rho^2}$$

Generated simulation datasets of a single emitter.  
Isolated spatial location of neutrals in plume.

Binned neutrals in RZ-space and generated a distribution of neutral density as a function of radial distance from centerline and parallel distance to emitter.

Hypothesized 1-dimensional functional forms for neutral density along profiles.



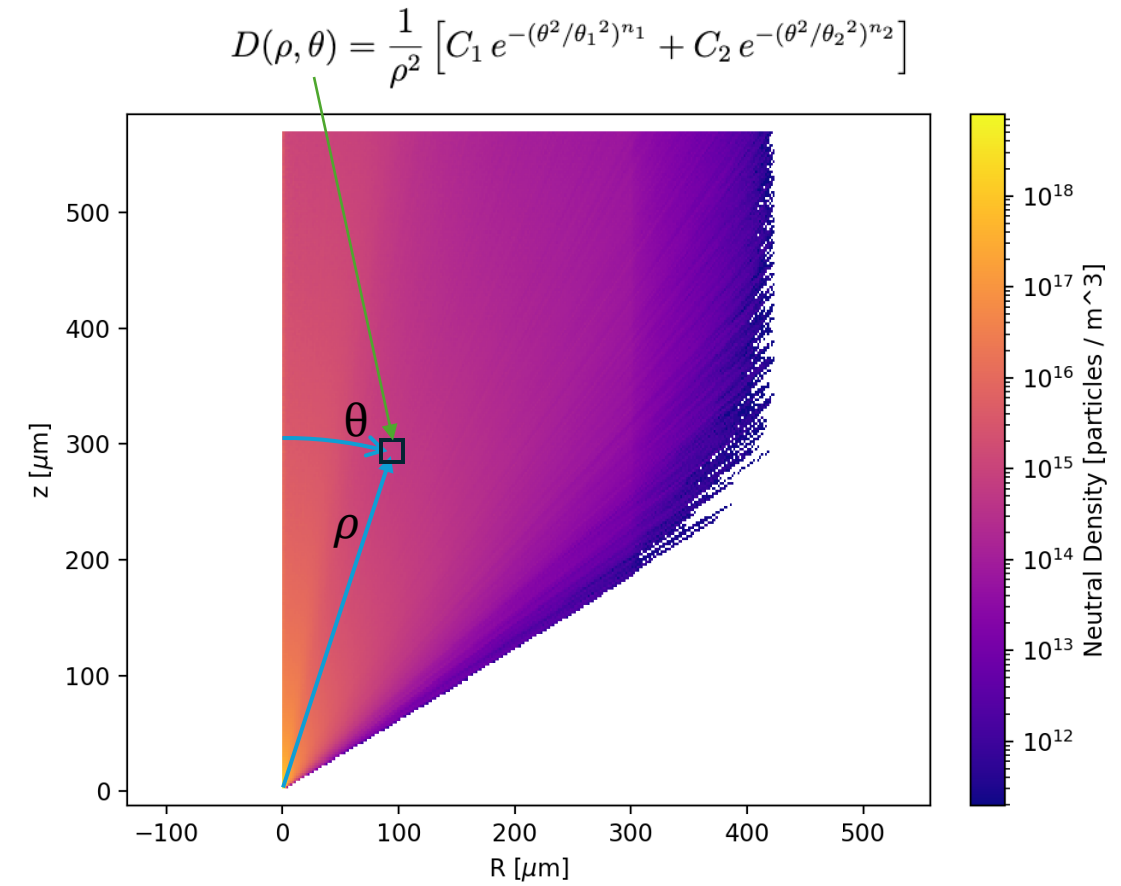
$$D(\theta) = C_1 e^{-(\theta^2/\theta_1^2)^{n_1}} + C_2 e^{-(\theta^2/\theta_2^2)^{n_2}}$$

# Methodology: two-dimensional functional form for single emitter

Combined Two 1-dimensional functional forms into one 2-dimensional functional form.

Used 2-dimensional functional form to predict neutral densities in 2-dimensions.

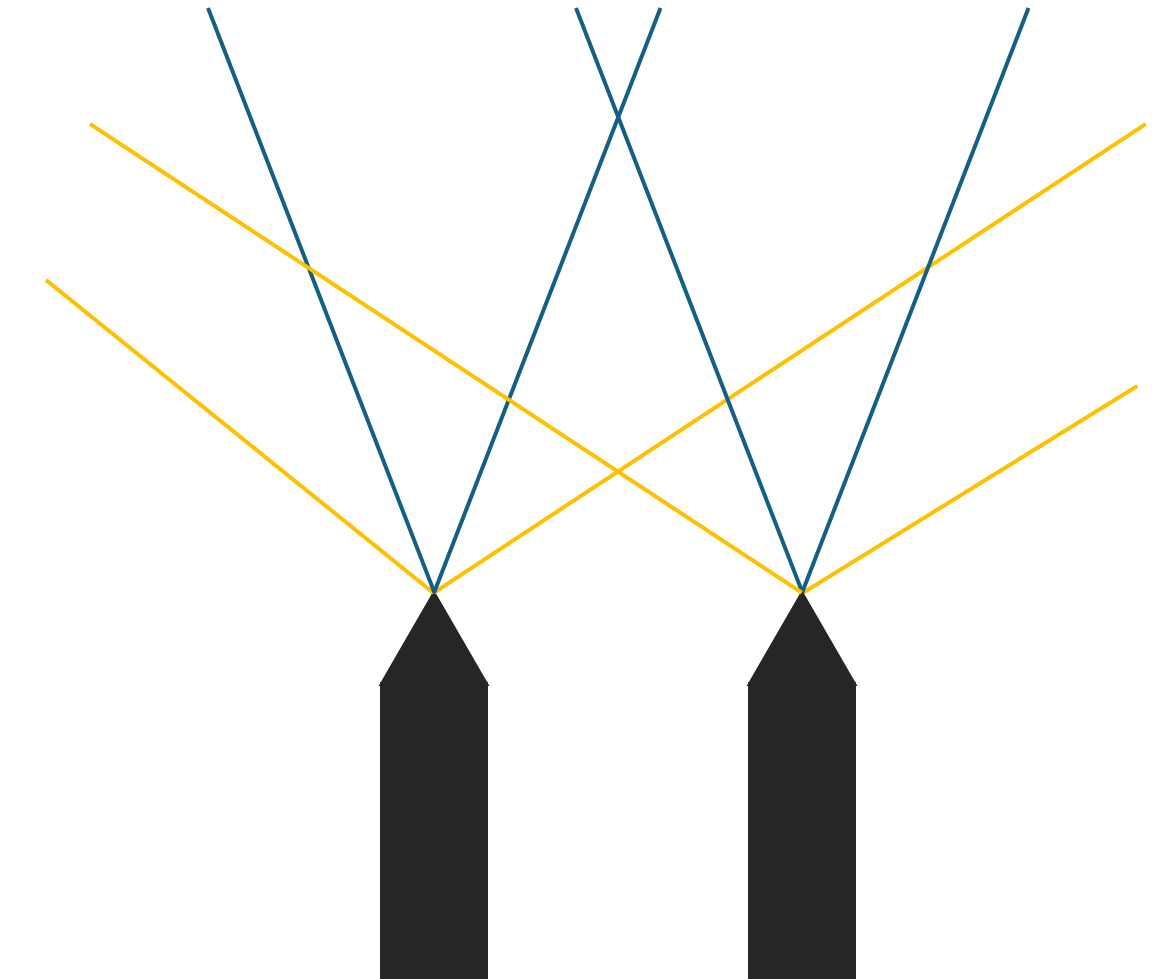
Used Python to fit the two-dimensional functional form to an emitter operating at different voltage conditions.



# Methodology: generate density distribution behind array

Generated a hexagonal grid of points to define the location of each emitter.

Used the fitted model to sum the contributions of each emitter in a plane orthogonal to the plane of the emitter.



**Results: Single Emitter**  
Distribution of neutrals behind a single emitter

# Model of neutral density behind a single emitter

- Two areas of high neutral density – Core and Wing

From 2 – 10 cm away from emitter:

- $D_{\text{core}} \approx 10^{12} \rightarrow 10^{10}$  Particles/m<sup>3</sup>
- $D_{\text{wing}} \approx 10^{11} \rightarrow 10^8$  Particles/m<sup>3</sup>
- $D < 10^7$  Particles/m<sup>3</sup> elsewhere

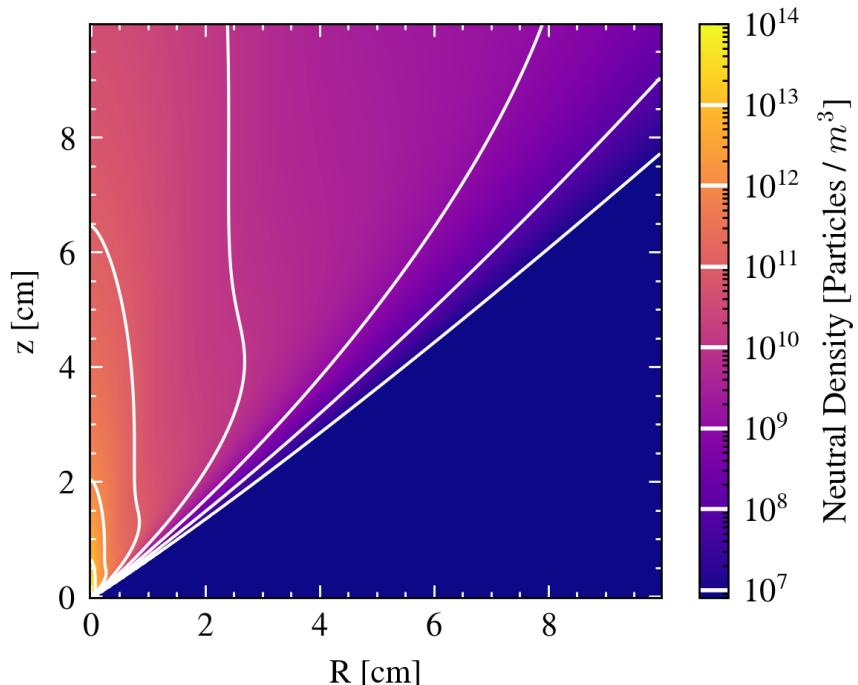


Figure 3. Model of neutral density behind a single emitter at 1600 V.

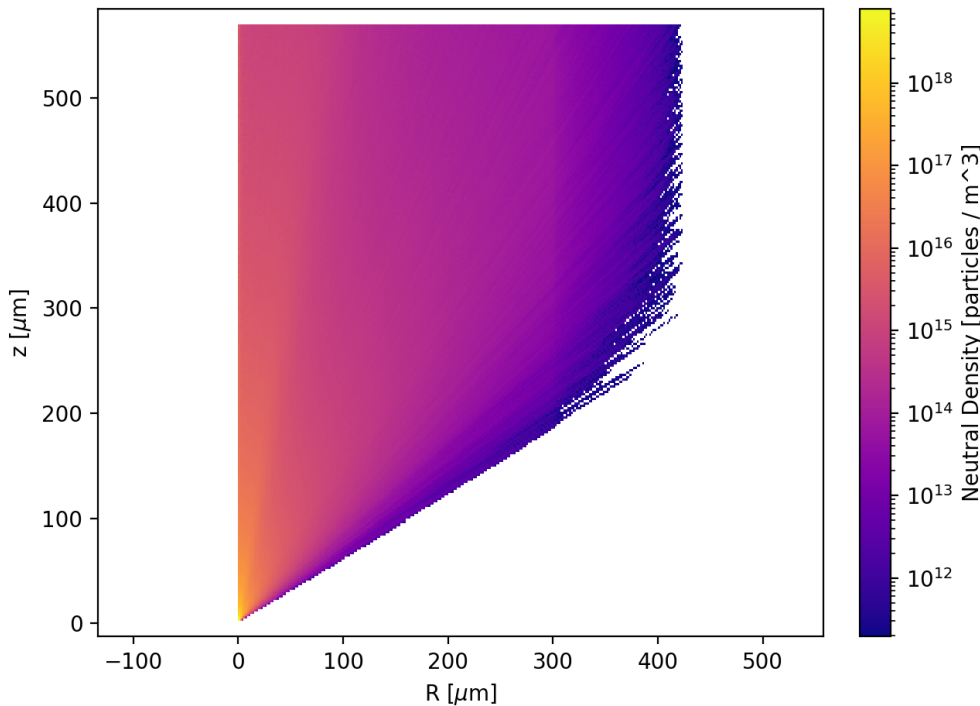


Figure 4. Raw simulation data at 1600 V.

# Accuracy of model near emitter

- Greater prediction accuracy in the wing
- Functional form  $1/\rho^2$  assumes no fragmentation behavior in the plume
- In core, model overpredicts neutral density since ions in core continue to fragment.
- Ions in wing do not stay there for long because of electric field.

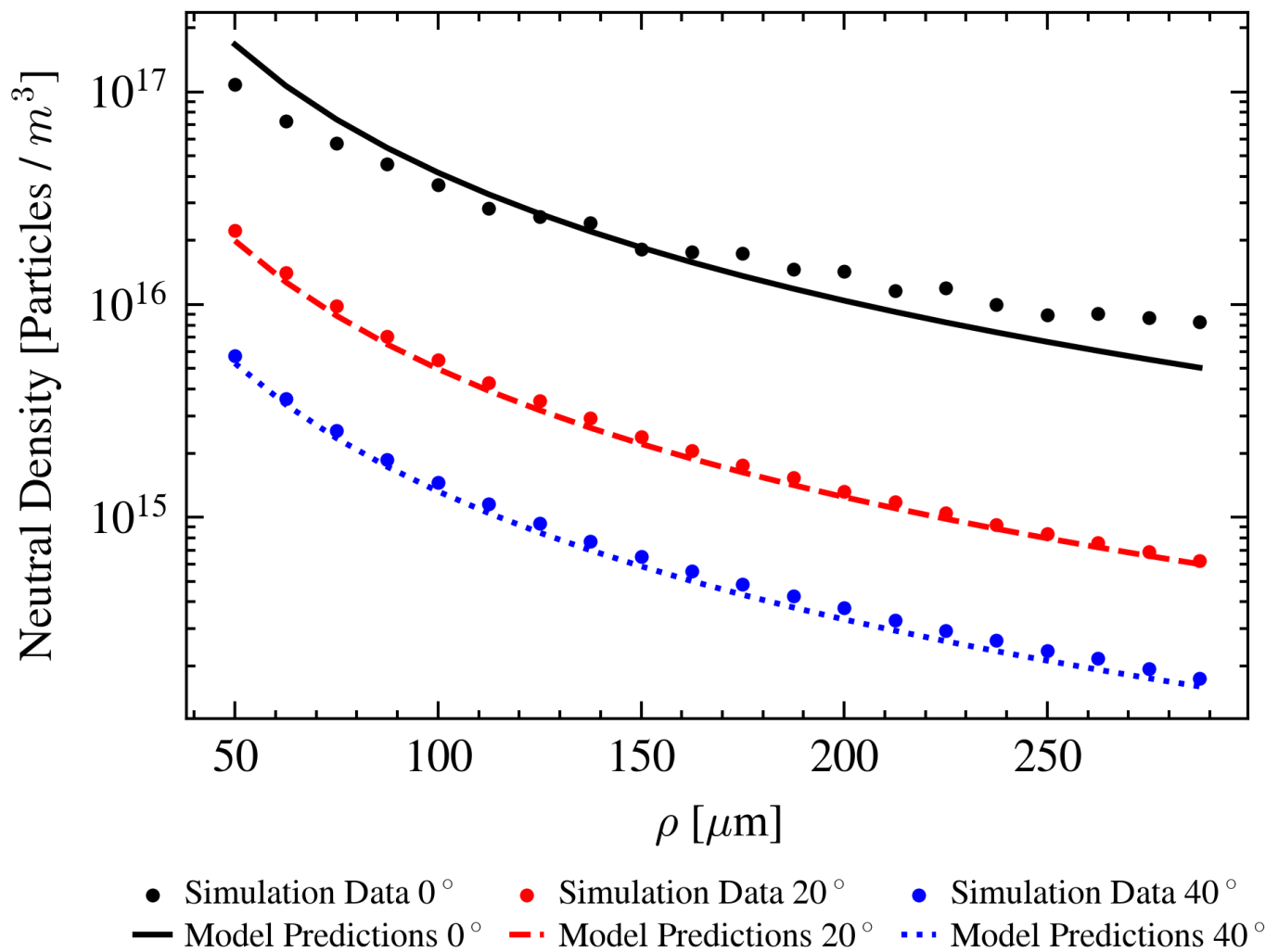


Figure 5. Comparison of Model Predictions and Simulation Data at 1600 V.

## Results: Voltage Dependence

Characterization of neutral density at different voltage conditions

# Neutral density behind a single emitter at low, medium, and high voltages

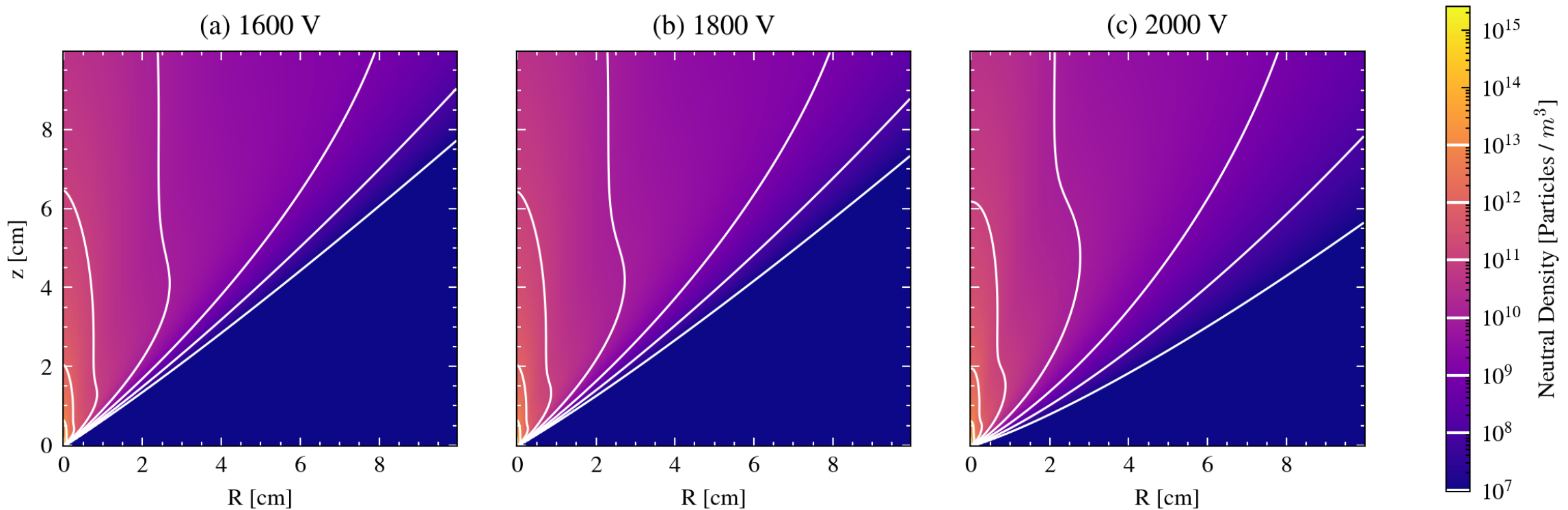


Figure 6. RZ heatmaps of neutral density behind a single emitter. (a) Distribution at 1600 V. (b) Distribution at 1800V. (c) Distribution at 2000V.

- **Voltage** has **small to moderate** effect on overall distribution (neutral density does not change by orders of magnitude anywhere in plume).

# Neutral density behind a single emitter at low, medium, and high voltages

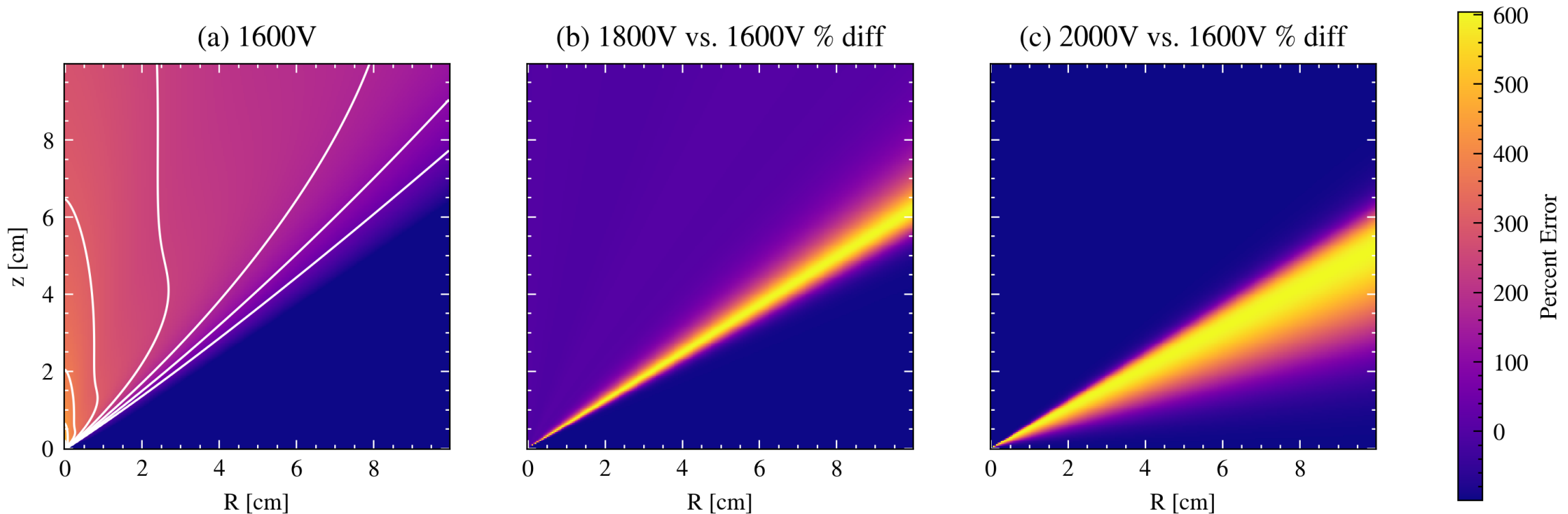


Figure 7. Comparison of neutral distributions at different voltage conditions. (a) Original heatmap of neutral density behind emitter at 1600V. (b) Percent difference between 1600 V heatmap and 1800 V heatmap. (c) Percent difference between 1600V heatmap and 2000 V heatmap.

- Moderate **increase** in neutrals at far end of wing as voltage **increases**

# Core vs. wing neutral density and their proportion as a function of voltage

- As **voltage increases**, there is a **lower proportion** of neutrals in the core compared to the far-wing.
- Greater fragmentation frequency at higher electric fields.
- Neutrals that fragment soon after emission from ions emitted from an off-axis emission site will stay in wing.

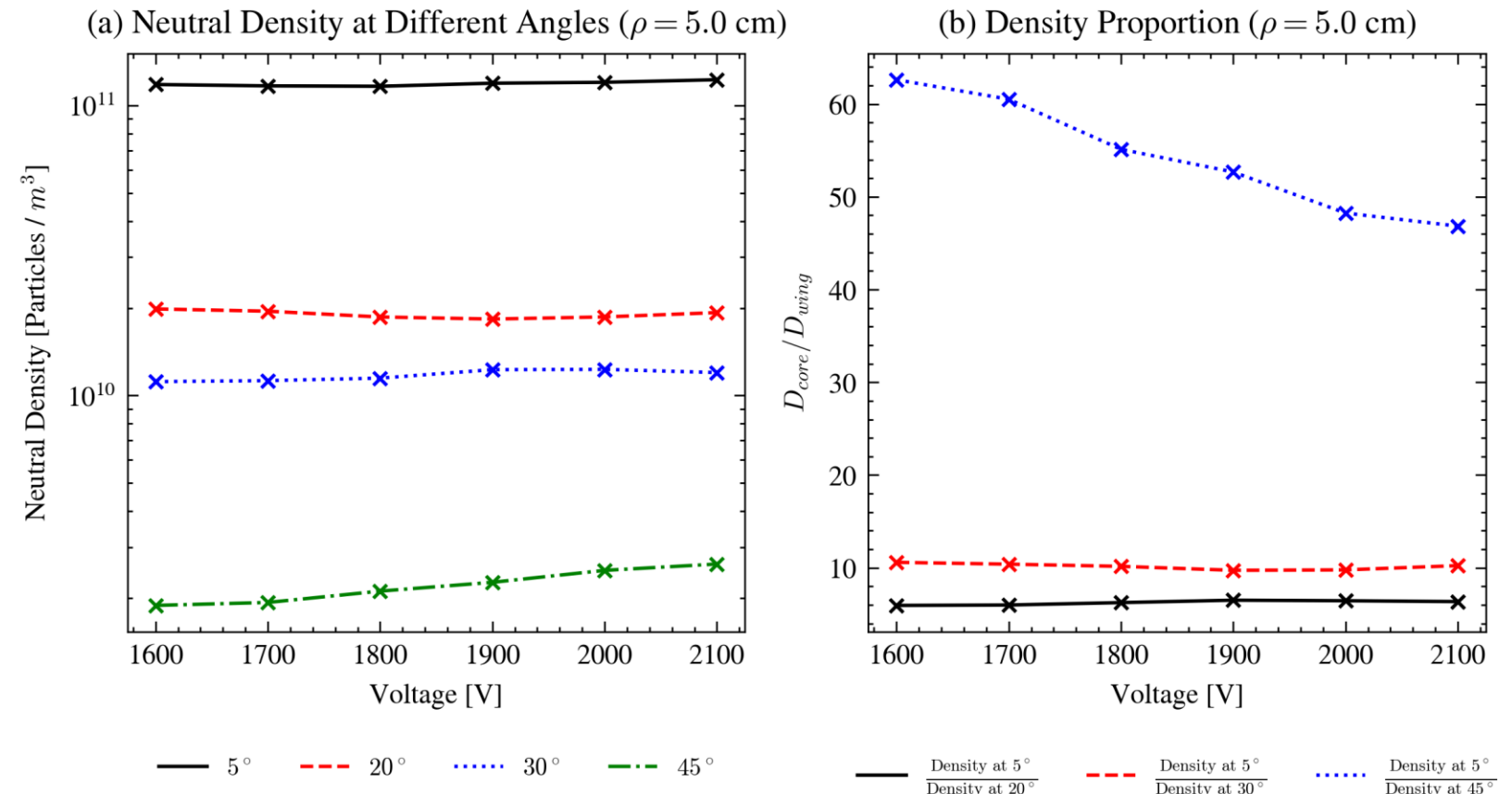


Figure 8. Neutral density in core versus neutral density in wing at  $\rho = 5 \text{ cm}$ .

# Cause of greater neutral density at edge of wing?

- Ions are emitted off-axis into the plume and are accelerated into the core of the plume.
- At higher voltages, the electric field is higher, so fragmentation effects occur more frequently.
- At higher voltages, ions that are emitted off-axis fragment sooner, so more neutrals travel at high angles from centerline.

# Neutral density behind a single emitter at low, medium, and high voltages

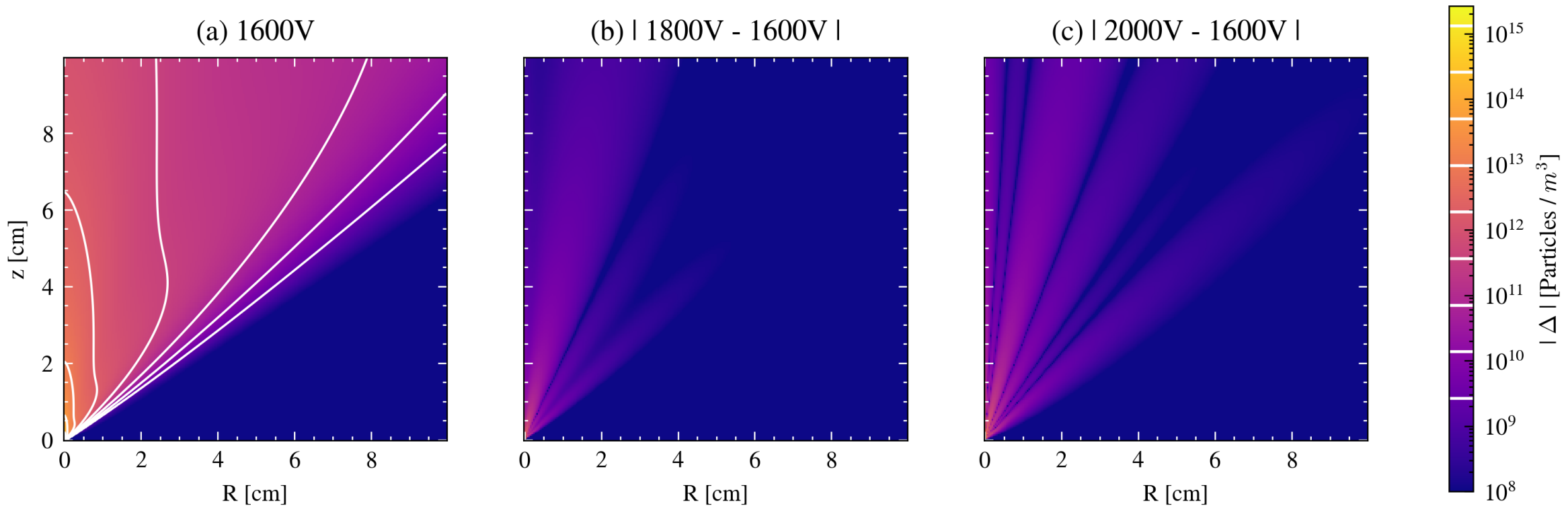


Figure 9. Comparison of neutral distributions at different voltage conditions. (a) Original heatmap of neutral density behind emitter at 1600V. (b) 1600 V heatmap subtracted from 1800 V heatmap. (c) 1600 V heatmap subtracted from 2000 V heatmap.

- **Voltage increases density** of neutrals in core and wing.
- **Larger increase** in neutral density at higher voltages.

# Neutral density profile dependence on voltage

- Neutral **density in core** is roughly **one order of magnitude greater** than neutral density in the **wing**.
- Neutral density at different voltages are **well within an order of magnitude of each other**.
- Spatial structure changes modestly. **Absolute density** increases but **remains within an order of magnitude**.

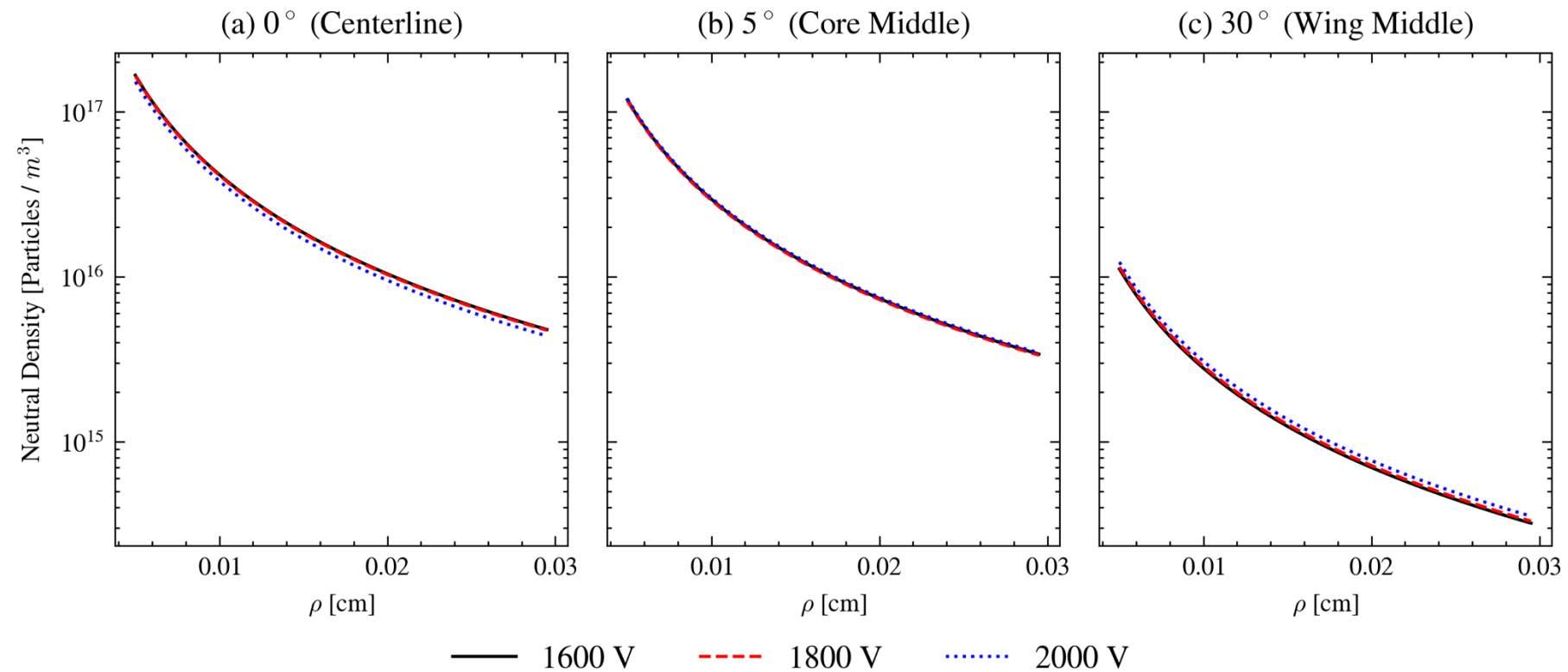


Figure 11. Neutral density as a function of distance from the emitter at different voltage conditions and angles from centerline.

## Results: Emitter Arrays

Neutral density distribution behind an array of emitters

# Neutral density behind an array of emitters

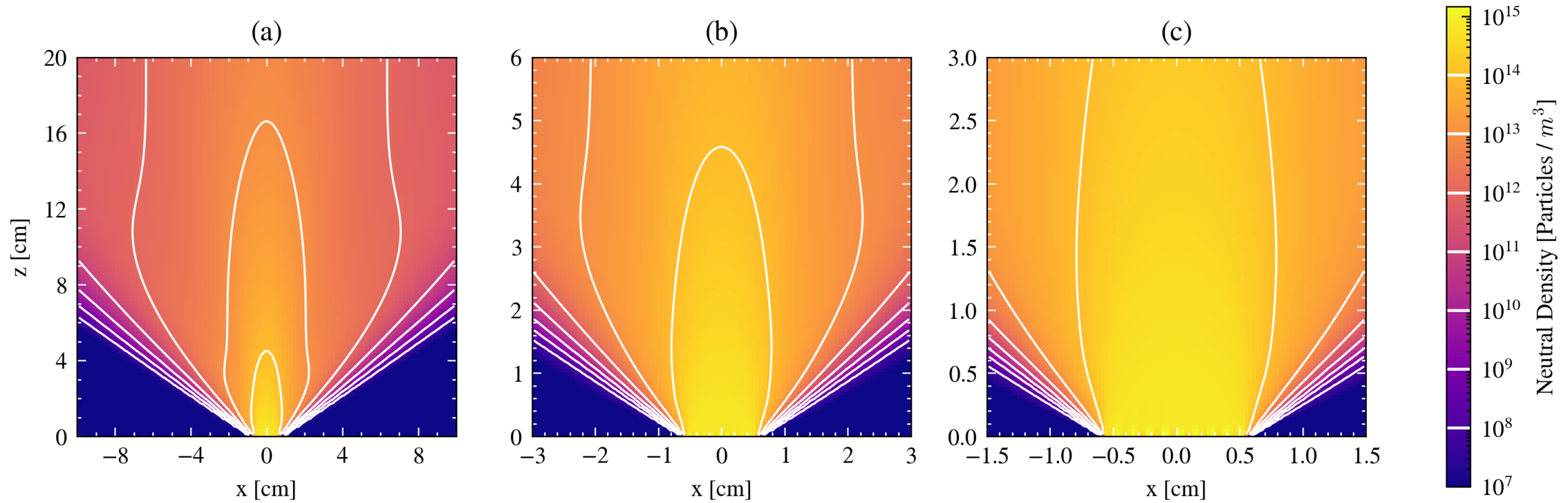


Figure 12. Neutral Density behind an Array of Emitters. (a) Far-out image (20 cm x 20 cm). (b) Medium-sized image (6 cm x 6 cm). (c) Close image (3 cm x 3 cm)

- Heatmaps display neutral density behind an array of emitters.
- Neutral density evaluated on a plane orthogonal to the plane of the array.

# Neutral density behind an array at low, medium, and high voltages

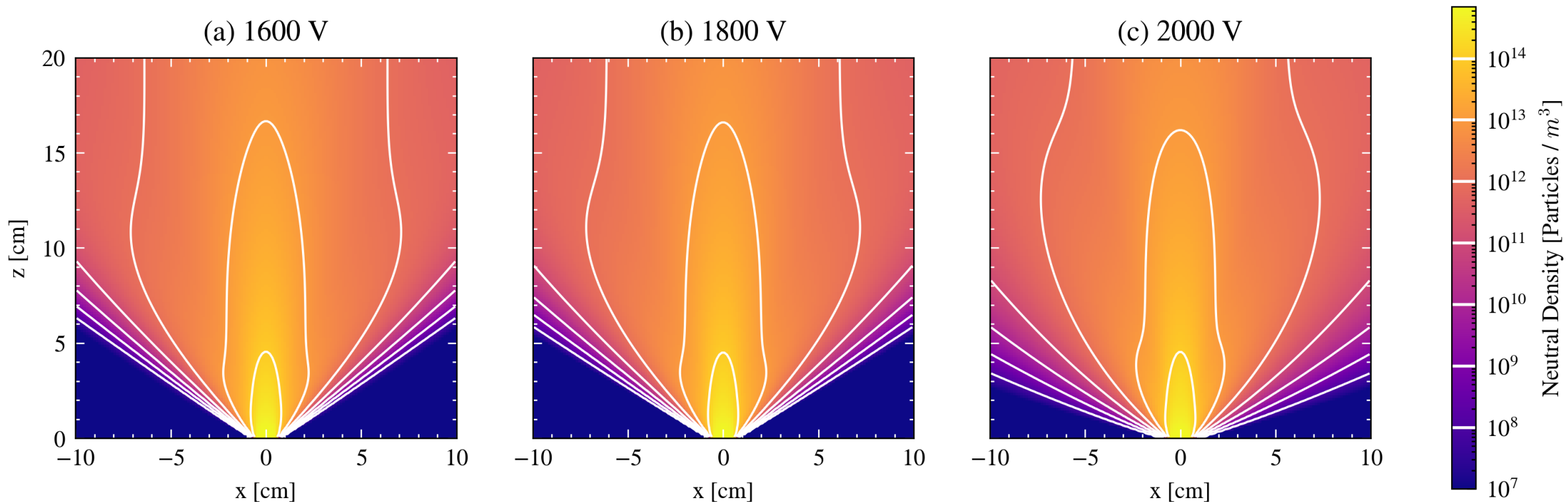


Figure 13. Model predictions of neutral density behind an array at (a) 1600 V, (b) 1800 V, (c) 2000V. Emitter pitch = 400  $\mu\text{m}$ , array size = (25 emitters x 28 emitters), View = (20 cm x 20 cm).

- Distribution **trends in voltage** for a single emitter are **replicated** for an array.

## Future work

- Develop further quantitative metrics to assess the accuracy of the model compared to simulation data.
- Change beam current and voltage simultaneously in simulations to model the distribution of neutrals for practical operating conditions.
- Predict neutrals behind an array in three-dimensions and visualize the distribution.
- Investigate error on  $\theta = 0$  profile due to continuous fragmentation.

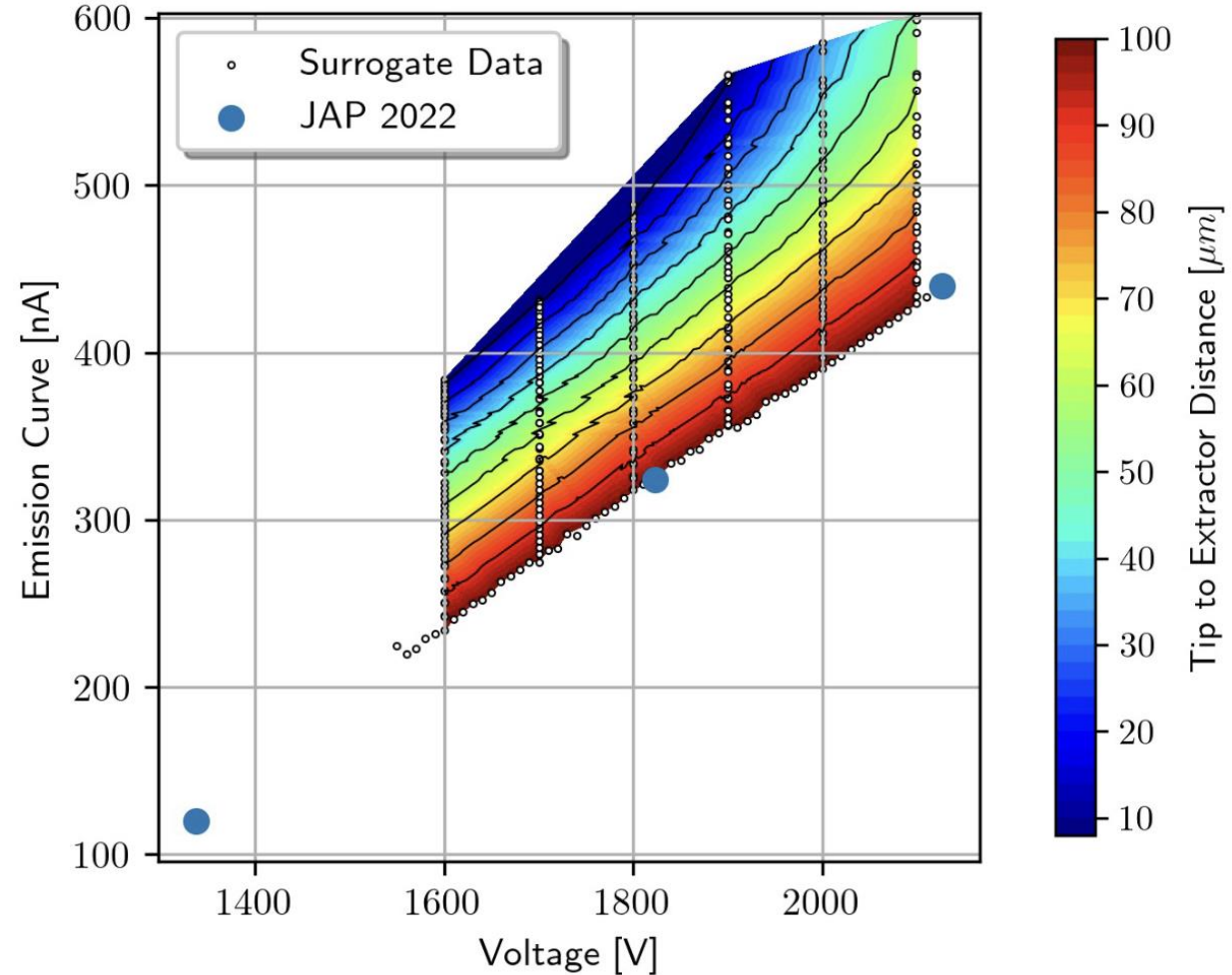


Figure 14. Emission curve [nA] as a function of voltage [V] at different tip to extractor distances.

# Conclusion

- The neutral density behind an emitter/array is **well fit** by the model:

$$D(\rho, \theta) = \frac{1}{\rho^2} \left[ C_1 e^{-(\theta^2/\theta_1^2)^{n_1}} + C_2 e^{-(\theta^2/\theta_2^2)^{n_2}} \right]$$

Where the power-law describes the density profile along a line at some angle to the z-axis, and the two supergaussians describe the profile along an arc at some distance from the emitter.

- **Higher voltage** result in a **larger** absolute **neutral density** in both the **core** and the **wing**. The **voltage** has the **largest effect** on the density of neutrals at **far edge of the wing**, which increases with voltage.
- Emitter **arrays** display **same trends** as **single emitters** in **neutral density** as voltage is swept.